MHD free convection boundary layer flow near the lower stagnation point flow of a horizontal circular cylinder in ferrofluid

IOP Conf. Series: Materials Science and Engineering **736** (2020) 022117 doi:10.1088/1757-899X/736/2/022117

MHD free convection boundary layer flow near the lower stagnation point flow of a horizontal circular cylinder in ferrofluid

S H M Yasin[1], M K A Mohamed[2], Z Ismail[1] & M Z Salleh[1]

[1] Centre for Mathematical Sciences, College of Computing and Applied Sciences, Universiti Malaysia Pahang, 26300 Gambang, Kuantan, Pahang, Malaysia
[2] School of Foundation and Inter Disciplinary Studies, DRB-HICOM University of Automotive Malaysia, Peramu Jaya Industrial Area, 26607 Pekan, Pahang, Malaysia

zuki@ump.edu.my

Abstract. The present numerical solution is to theoretically investigate the magnetohydrodynamic (MHD) free convection boundary layer flow and the heat transfer of ferrofluid near the lower stagnation point of a horizontal circular cylinder. The conventional heat transfer of fluids such as water and oil is inherently the poor heat transfer performance. Nanofluid which is formed by magnetic nanoparticles is known as ferrofluid and has shown a particular achievement when the effect of external magnetic is applied. For this purpose, ferrofluid that contains magnetite, Fe_3O_4 and water are considered. The dimensional governing equations are transformed by using non-dimensional variables and non-similar transformations to form nonlinear partial differential equations. The numerical solution using the implicit finite difference scheme namely Keller-box method is used to solve the nonlinear partial differential equations. Numerical results on velocity and temperature distributions as well as the quantity of interest of pertinent parameters such as magnetic parameter and the volume fraction of ferroparticles parameter are discussed. It is noticeable that the reduced Nusselt number of ferrofluid decreases through the increase of magnetic parameter strength.

1. Introduction

The discovery of the term nanofluid that is first introduced by Choi and Eastman [1] shows that the nanoparticles added in the conventional base fluid exhibit high thermal conductivity and enhance the heat transfer. Based on material type, nanofluid is classified as metallic nanoparticles (Cu, Al, Fe, Au and Ag) and non-metallic nanoparticles (Al_2O_3, CuO, Fe_3O_4, TiO_2 and SiC). Magnetic nanofluid which is also known as ferrofluid has been widely investigated in theoretical [2-4] and experimental studies [5-7] because of its incredible outcomes on thermal conductivity. Ferrofluid contains magnetic nanoparticles (ferroparticles) such as magnetite (Fe_3O_4), hematite (Fe_2O_3), cobalt ferrite ($CoFe_2O_4$) and other compound with iron oxides which suspended in a liquid carrier like water, oil, ethylene glycol and so forth. According to Papell [8], despite the presence of various magnetic nanofluid materials, magnetite (Fe_3O_4) has been found to be the most satisfactory in practice.

The component of ferrofluid contains approximately 85% volume of base fluid, 5% volume of magnetic nanoparticles and 10% volume of surfactants [9]. Ferrofluid exhibits superparamagnetism which means the magnetic field consists of ferromagnetic with no long-range order between particles

[10, 11]. Subsequently, ferrofluid becomes strongly magnetized in the presence of magnetic field that provides low viscosity, easy flowability and low energy. The flow of ferrofluid through the surface can be controlled with the presence of magnetic field and it also has the ability to prevent the devices or equipment from overheating and reduce clogging. Ferrofluid has been utilized in many technological industries such as in sealing hard drives, rotating shafts, rotating X-ray tubes, rods and sink float systems for separation of materials, lubricating bearing and dumpers, as well as heating controller in electric motors and speakers. The fluid characteristics and heat transfer have different performance and outcomes when the fluid flows at different geometries such as flat plate, inclined plate, stretching or shrinking sheet, wedge, horizontal circular cylinder and sphere [12]. It should be noted that the geometry of interest in this study is the horizontal circular cylinder.

Joshi and Sukhatme [13], Merkin [14], Merkin and Pop [15] are among the pioneers who studied the boundary layer flow of free, forced and mixed convection in viscous fluid over a horizontal circular cylinder. After a few years, Aldoss et al. [16] investigated the magnetohydrodynamic (MHD) mixed convection of viscous fluid over a horizontal circular cylinder and found the presence of magnetic field leads to the decrease of velocity field, local wall shear stress and local Nusselt number as well as an increased value of temperature. The idea is then extended by Aldos and Ali [17], who considers the effects of suction and blowing on MHD force and free convection from a horizontal circular cylinder. The observation on the wall shear stress and Nusselt number showed a prominent decrease with the application of magnetic field. However, there are some drawbacks of viscous fluid flow over a horizontal circular cylinder in terms of sedimentation, surface abrasion and thermal conductivity.

Since Choi and Eastman [1] discovered the significant increase in thermal conductivity of liquid dispersant with nanoparticles, the studies of nanofluid have attracted interests from many researchers lately. Recently, the studies of convective flow over a horizontal circular cylinder in nanofluid have been carried out by Tlili et al.[18], Mahat et al. [19], Reddy and Chamkha [20], Mohamed et al. [21] and Mabood et al. [22] who have solved the nanofluid flow and heat transfer problems. There are two different nanofluid models which are constantly used by the researchers to study the Brownian motion and the thermophoresis on heat transfer characteristics namely Buongiorno model [23] and Tiwari and Das model [24] that focus on the behaviour of nanofluid. Reddy and Chamkha [20] conducted the numerical solution by using Buongiorno model [23] and finite-element method for free convection boundary layer flow and found that an upsurge of buoyancy ratio parameter leads to the decline of the reduced Nusselt number. Besides, the increment in Brownian motion parameter elevates the reduced Nusselt number but when the thermophoresis motion parameter increases, the reduced Nusselt number declines. However, different results were obtained by Mohamed et al. [21] where the reduced Nusselt number decreases as Brownian motion and the thermophoresis motion increases. Mahat et al. [19] and Mabood et al. [22] applied the Tiwari and Das model [24] and finite difference method for mixed and forced convection respectively. Mahat et al. [19] explored the effect of viscous dissipation but did not discuss the volume fraction of Cu nanoparticles in details and concluded that the reduced Nusselt number decreases with an increase of the value of the Eckert number. Meanwhile, Mabood et al. [22] explained that the reduced Nusselt number increases with an increase in the volume fraction of Cu and Al_2O_3 nanoparticles. Most of the earlier studies considered copper (Cu), alumina (Al_2O_3) and titania (TiO_2) as nanoparticles materials in their numerical studies.

The studies mentioned above gave an idea and inspired the authors to the investigation of free convection ferrofluid flows at a lower stagnation point of a horizontal circular cylinder. This investigation also considered the magnetohydrodynamic (MHD) flow because of the ferrofluid characteristics change in the presence of a magnetic field. This present study is undertaken to estimate the trend of ferrofluid flow and heat transfer at different values magnetic parameter and ferroparticle volume fraction. The stable colloidal suspension of magnetite (Fe_3O_4) nanoparticles and water as a carrier fluid also have been considered. The Tiwari and Das model [24] is implemented to investigate this problem and numerically solve it by applying an implicit finite difference scheme which is known as the Keller-box method.

2. Mathematical formulation

Consider a steady, two-dimensional laminar free convection boundary layer flows of incompressible ferrofluid over a horizontal circular cylinder. A horizontal circular cylinder of radius a, which is heated to a constant temperature, T_w embedded in a ferrofluid with ambient temperature, T_∞ and free stream velocity, U_∞ as shown in figure 1. The orthogonal coordinates of $\bar{x}$ and $\bar{y}$ are measured along the cylinder surface, starting with the lower stagnation point, $\bar{x}=0$ and normal to it, respectively. Further, a uniform magnetic field of strength, B_o is assumed applied normal on the cylinder surface. The magnetic Reynolds number is assumed small, and thus the induced magnetic field is negligible. Both the base fluid and ferroparticles are assumed to be in thermal equilibrium. The cylinder surface is subjected to a constant wall temperature and no slip velocity condition is considered. Under the assumptions that the boundary layer approximation is valid, the dimensional governing equations of laminar and steady free convection boundary layer flow are [25-27]:

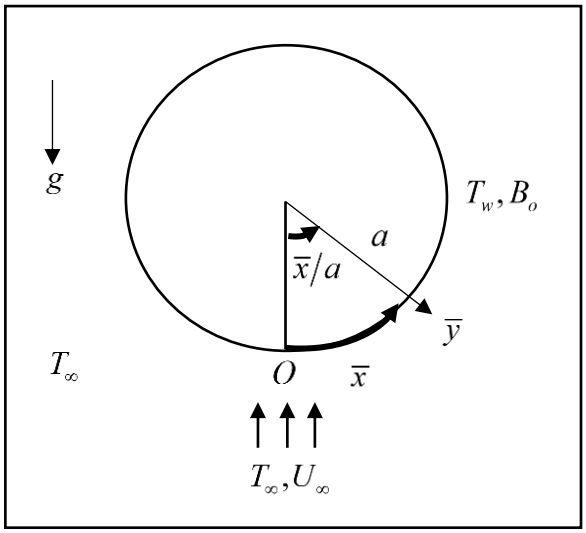

Figure 1. Physical model and coordinate system

$$\frac{\partial \bar{u}}{\partial \bar{x}}+\frac{\partial \bar{v}}{\partial \bar{y}}=0, \tag{1}$$

$$\bar{u}\frac{\partial \bar{u}}{\partial \bar{x}}+\bar{v}\frac{\partial \bar{u}}{\partial \bar{y}}=\nu_{ff}\frac{\partial^2 \bar{u}}{\partial \bar{y}^2}+\frac{(\rho\beta)_{ff}}{\rho_{ff}}g\left(T-T_\infty\right)\sin\frac{\bar{x}}{a}-\frac{\sigma_{ff}B_o^2}{\rho_{ff}}\bar{u}, \tag{2}$$

$$\bar{u}\frac{\partial T}{\partial \bar{x}}+\bar{v}\frac{\partial T}{\partial \bar{y}}=\alpha_{ff}\frac{\partial^2 T}{\partial \bar{y}^2} \tag{3}$$

subject to the boundary conditions

$$\begin{aligned}&\bar{u}(\bar{x},0)=\bar{v}(\bar{x},0)=0,\ T(\bar{x},0)=T_w \text{ at } \bar{y}=0\\ &\bar{u}(\bar{x},\infty)\to 0,\ T(\bar{x},\infty)\to T_\infty \text{ as } \bar{y}\to\infty\end{aligned} \tag{4}$$

where $\bar{u}$ and $\bar{v}$ indicates the velocity components along the $\bar{x}$ and $\bar{y}$ axes, respectively. Further, the subscripts *ff*, *f* and *s* respectively referring to ferrofluid, base fluid and ferroparticles. ν is the kinematic viscosity, μ is the dynamic viscosity, ρ is the density, g is the gravity acceleration, σ is the electrical conductivity, β is the ferrofluid thermal expansion, T is local temperature, $\left(\rho C_p\right)$ is the effective heat capacity and α is the thermal diffusivity which can be expressed in terms of the volume fraction ϕ as follows [25, 28, 29]:

$$\begin{gathered}\nu_{ff}=\frac{\mu_{ff}}{\rho_{ff}},\ \rho_{ff}=(1-\phi)\rho_f+\phi\rho_s,\ \ \mu_{ff}=\frac{\mu_f}{(1-\phi)^{2.5}},\ \ \left(\rho\beta\right)_{nf}=(1-\varphi)\left(\rho\beta\right)_f+\varphi\left(\rho\beta\right)_s,\\ \alpha_{ff}=\frac{k_{ff}}{\rho_{ff}\left(C_p\right)_{ff}},\quad \frac{\sigma_{ff}}{\sigma_f}=1+\frac{3\left(\frac{\sigma_s}{\sigma_f}-1\right)\phi}{\left(\frac{\sigma_s}{\sigma_f}+2\right)-\left(\frac{\sigma_s}{\sigma_f}-1\right)\phi},\quad \left(\rho C_p\right)_{ff}=(1-\phi)\left(\rho C_p\right)_f+\phi\left(\rho C_p\right)_s.\end{gathered} \tag{5}$$

where k represents the thermal conductivity and can be defined as

$$\frac{k_{ff}}{k_f}=\frac{k_s+2k_f-2\phi(k_f-k_s)}{k_s+2k_f+\phi(k_f-k_s)}. \tag{6}$$

Note that the thermophysical properties of base fluid (water) and ferroparticles (magnetite) have been listed in table 1.

Table 1. Thermophysical properties of base fluid and ferroparticles [30, 31].

Physical Properties	Water	Magnetite (Fe_3O_4)
ρ (kg/m^3)	997.1	5200
C_p (J/kg·K)	4179	670
k (W/m·K)	0.613	6
$\sigma\left(\Omega^{-1}\mathrm{m}^{-1}\right)$	0.05	25000
β (1/K)	0.00021	0.000013

Next, the governing non-dimensional variables are introduced:

$$x=\frac{\bar{x}}{a},\quad y=Gr^{1/4}\frac{\bar{y}}{a},\quad u=\frac{a}{\nu_f}Gr^{-1/2}\bar{u},\quad v=\frac{a}{\nu_f}Gr^{-1/4}\bar{v},\quad \theta(\eta)=\frac{T-T_\infty}{T_w-T_\infty}. \tag{7}$$

where θ is the rescaled dimensionless temperature of the fluid and $Gr=\dfrac{g\beta_f(T_w-T_\infty)a^3}{\nu_f{}^2}$ is the Grashof number. Using variables (7) and definitions (5) and (6), equations (1) to (3) becomes

$$\frac{\partial u}{\partial x}+\frac{\partial v}{\partial y}=0, \tag{8}$$

$$u\frac{\partial u}{\partial x}+v\frac{\partial u}{\partial y}=\frac{\nu_{ff}}{\nu_f}\frac{\partial^2 u}{\partial y^2}+\frac{(1-\phi)\rho_f+\phi\left(\rho\beta\right)_s/\beta_f}{(1-\phi)\rho_f+\phi\rho_s}\theta\sin x-\frac{\sigma_{ff}}{\sigma_f\left((1-\phi)+\phi\left(\rho_s/\rho_f\right)\right)}Mu, \tag{9}$$

$$u\frac{\partial \theta}{\partial x}+v\frac{\partial \theta}{\partial y}=\frac{k_{ff}/k_f}{(1-\phi)+\phi(\rho C_p)_s/(\rho C_p)_f}\frac{1}{\Pr}\frac{\partial^2\theta}{\partial y^2}, \tag{10}$$

subject to the boundary conditions

$$\begin{gathered}u(x,0)=0,\ v(x,0)=0,\ \theta(x,0)=1,\\ u(x,\infty)\to 0,\ \ \theta(x,\infty)\to 0\end{gathered} \tag{11}$$

where $M=\dfrac{\sigma_f a^2 B_o{}^2(x)}{\nu_f\rho_f Gr^{1/2}}$ is the magnetic parameter and $\Pr=\dfrac{\nu_f\left(\rho C_p\right)_f}{k_f}$ is the Prandtl number. In order to solve equations (8) to (10), the following functions are introduced:

$$\psi=xf(x,y),\quad \theta=\theta(x,y), \tag{12}$$

where ψ is the stream function defined as $u=\dfrac{\partial\psi}{\partial y}$ and $v=-\dfrac{\partial\psi}{\partial x}$ which identically satisfies equation (8). Substitute equation (12) into equation (9) and (10), the following partial differential equations are obtained:

$$\begin{gathered}\frac{1}{(1-\phi)^{2.5}\left[1-\phi+(\phi\rho_s)/(\rho_f)\right]}\frac{\partial^3 f}{\partial y^3}+f\frac{\partial^2 f}{\partial y^2}-\left(\frac{\partial f}{\partial y}\right)^2+\frac{(1-\phi)\rho_f+\phi\left(\rho\beta\right)_s/\beta_f}{(1-\phi)\rho_f+\phi\rho_s}\frac{\sin x}{x}\theta\\ -\frac{\sigma_{ff}/\sigma_f}{\left(1-\phi\right)+\phi\left(\rho_s/\rho_f\right)}M\frac{\partial f}{\partial y}=x\left(\frac{\partial f}{\partial y}\frac{\partial^2 f}{\partial x\partial y}-\frac{\partial f}{\partial x}\frac{\partial^2 f}{\partial y^2}\right),\end{gathered} \tag{13}$$

$$\frac{k_{ff}/k_f}{(1-\phi)+\phi(\rho C_p)_s/(\rho C_p)_f}\frac{1}{\Pr}\frac{\partial^2\theta}{\partial y^2}+f\frac{\partial\theta}{\partial y}=x\left(\frac{\partial f}{\partial y}\frac{\partial\theta}{\partial x}-\frac{\partial f}{\partial x}\frac{\partial\theta}{\partial y}\right). \tag{14}$$

The boundary conditions (10) becomes:

$$\begin{gathered}f(x,0)=0,\ \ \frac{\partial f}{\partial y}(x,0)=0,\ \ \theta(x,0)=1,\\ \frac{\partial f}{\partial y}(x,\infty)\to 0,\ \ \theta(x,\infty)\to 0,\end{gathered} \tag{15}$$

It is worth mentioning that the lower stagnation point of a horizontal circular cylinder when $x\approx 0$, the equations (13) and (14) are reduced to the following ordinary differential equations that the f' and θ' denotes the differentiation with respect to the variable y.

$$\frac{1}{(1-\phi)^{2.5}\left[1-\phi+(\phi\rho_s)/(\rho_f)\right]} f''' + ff'' - f'^2 + \frac{(1-\phi)\rho_f + \phi(\rho\beta)_s/\beta_f}{(1-\phi)\rho_f + \phi\rho_s}\theta - \frac{\sigma_{ff}/\sigma_f}{(1-\phi)+\phi(\rho_s/\rho_f)} Mf' = 0, \tag{16}$$

$$\frac{k_{ff}/k_f}{(1-\phi)+\phi(\rho C_p)_s/(\rho C_p)_f}\frac{1}{\Pr}\theta'' + f\theta' = 0. \tag{17}$$

and the boundary conditions:

$$\begin{gathered} f(0)=0, \quad f'(0)=0, \quad \theta(0)=1, \\ f'(\infty)\to 0, \quad \theta(\infty)\to 0, \end{gathered} \tag{18}$$

The physical quantities of interest are the skin friction coefficient C_f and the local Nusselt number Nu_x are given by [32]:

$$C_f = \frac{\tau_w}{\rho_f u_\infty^2} \quad \text{and} \quad Nu_x = \frac{aq_w}{k_f(T_w - T_\infty)}, \tag{19}$$

The surface shear stress τ_w and the surface heat flux q_w are given by:

$$\tau_w = \mu_{ff}\left(\frac{\partial \bar{u}}{\partial \bar{y}}\right)_{\bar{y}=0} \quad \text{and} \quad q_w = -k_{ff}\left(\frac{\partial T}{\partial \bar{y}}\right)_{\bar{y}=0} \tag{20}$$

Using variables (7), definitions (5) and (6) as well the functions (12) turn into:

$$C_f Gr^{1/4} = \frac{1}{(1-\phi)^{2.5}}\left(x\frac{\partial^2 f}{\partial y^2}\right)_{y=0} \quad \text{and} \quad Nu_x Gr^{-1/4} = -\frac{k_{ff}}{k_f}\left(\frac{\partial \theta}{\partial y}\right)_{y=0} \tag{21}$$

Furthermore, the velocity profiles and temperature distributions at the lower stagnation point of horizontal circular cylinder can be obtained from the following relations:

$$u = f'(y) \text{ and } \theta = \theta(y), \tag{22}$$

3. Results and discussion

Keller-box method is used to numerically solve Eqs. (13) and (14) along with the constant wall temperature boundary conditions (15). This is the most preferred method because it is unconditionally stable and able to solve the partial differential equation problems in any order. The numerical codes are then programmed in Matlab software with the step size $\Delta x = 0.005$ and $\Delta x = 0.02$, and the boundary layer thickness $y_\infty = 8$. The comparison of present results of the reduced skin friction, $C_f Gr^{1/4}$ and the reduced Nusselt number, $Nu_x Gr^{-1/4}$ with the previously reported numerical results have been made to validate the numerical result obtained. Table 2 and table 3 shows the present results are found in good agreement with previous published results for various values of x when $M = \phi = 0$ and $\Pr = 1$. The

effect of ferroparticles volume fraction, ϕ and magnetic parameter, M towards velocity, temperature and reduced Nusselt number at the lower stagnation point, $x \approx 0$ of a horizontal circular cylinder with Prandtl number of water are taken at Pr = 6.2 and discussed below (figure 2 to 6). The volume fraction of ferroparticles ϕ is studied within the range of $0 \le \phi \le 0.1$ where $\phi = 0$ represent the pure fluid water.

Table 2. Comparison values of $C_f Gr^{1/4}$ with previously published results when $M = \phi = 0$ and $\Pr = 1$.

x	Merkin [14]	Azim [27]	Mohamed et al. [21]	Zokri et al. [33]	Present
0	0.0000	0.0000	0.0000	0.0000	0.0000
$\pi/6$	0.4151	0.4139	0.4121	0.4120	0.4121
$\pi/3$	0.7558	0.7528	0.7538	0.7507	0.7538
$\pi/2$	0.9579	0.9526	0.9563	0.9554	0.9563
$2\pi/3$	0.9756	0.9678	0.9743	0.9728	0.9743
$5\pi/6$	0.7822	0.7718	0.7813	0.7761	0.7813
π	0.3391	0.3239	0.3371	0.3301	0.3371

Table 3. Comparison values of $Nu_x Gr^{-1/4}$ with previously published results when $M = \phi = 0$ and $\Pr = 1$
.

x	Merkin [14]	Azim [27]	Mohamed et al. [21]	Zokri et al. [33]	Present
0	0.4214	0.4216	0.4214	0.4214	0.4214
$\pi/6$	0.4161	0.4163	0.4163	0.4162	0.4163
$\pi/3$	0.4007	0.4006	0.4008	0.4009	0.4008
$\pi/2$	0.3745	0.3742	0.3744	0.3743	0.3744
$2\pi/3$	0.3364	0.3356	0.3364	0.3363	0.3364
$5\pi/6$	0.2825	0.2811	0.2824	0.2814	0.2824
π	0.1945	0.1912	0.1939	0.1932	0.1939

Figure 2 depicts the magnetohydrodynamic flow while increasing the ferroparticles volume fraction towards the velocity of ferrofluid. The increment of ferroparticles volume fraction leads to a decline of the velocity of ferrofluid but then, increases until it approaches the free stream which causes it to elevate the momentum boundary layer thickness. According to the experiment results conducted by Malekzadeh et al. [34] and Toghraie et al. [7], the viscosity of magnetite, Fe_3O_4-water based increases with the increase of the ferroparticles volume fraction. However, temperature is one of the factors that influence the variations of dynamic viscosity [35]. Figure 3 shows that the increment in ferroparticles volume fraction elevates the temperature and thermal boundary layer. Obviously, figure 2 and 3 illustrate the correlation between viscosity and temperature when the ferroparticles volume fraction increases where figure 2 shows the velocity of ferrofluid is increases in parallel with the increase of the temperature (refer figure 3) due to the decline in ferrofluid viscosity. Similar results were reported in an experimental study by Malekzadeh et al. [34], Toghraie et al. [7] and Sundar et al. [36]. Physically, the high temperature that is applied to the fluid will cause the random motion of the molecule. Therefore, by weakening the intermolecular force of attraction, it will then reduce the viscosity of fluid and increase the velocity of fluid.

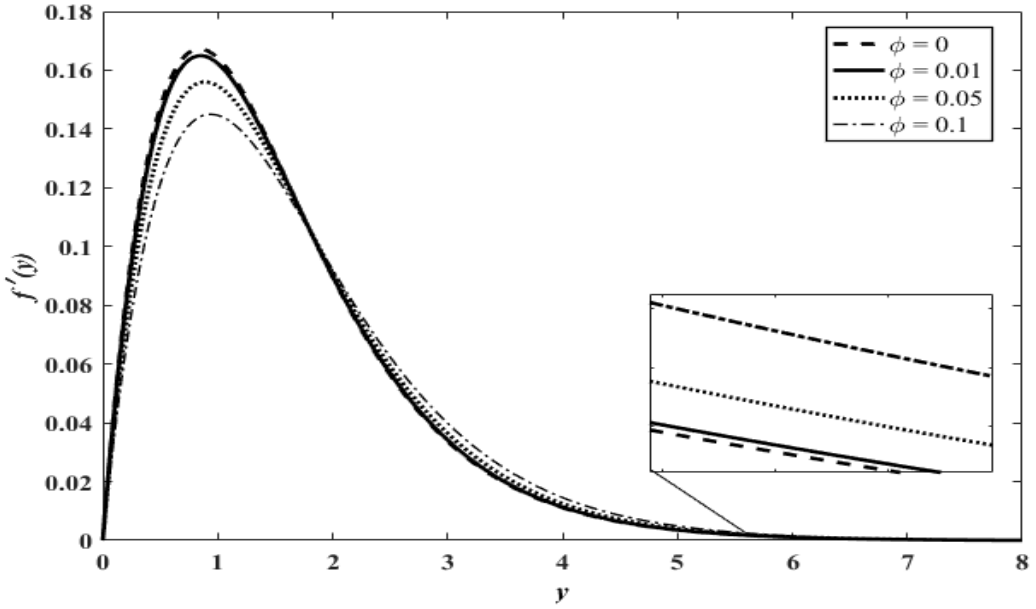

Figure 2. Velocity profile $f'(y)$, for increasing the ferroparticles volume fraction, ϕ when $M=1$.

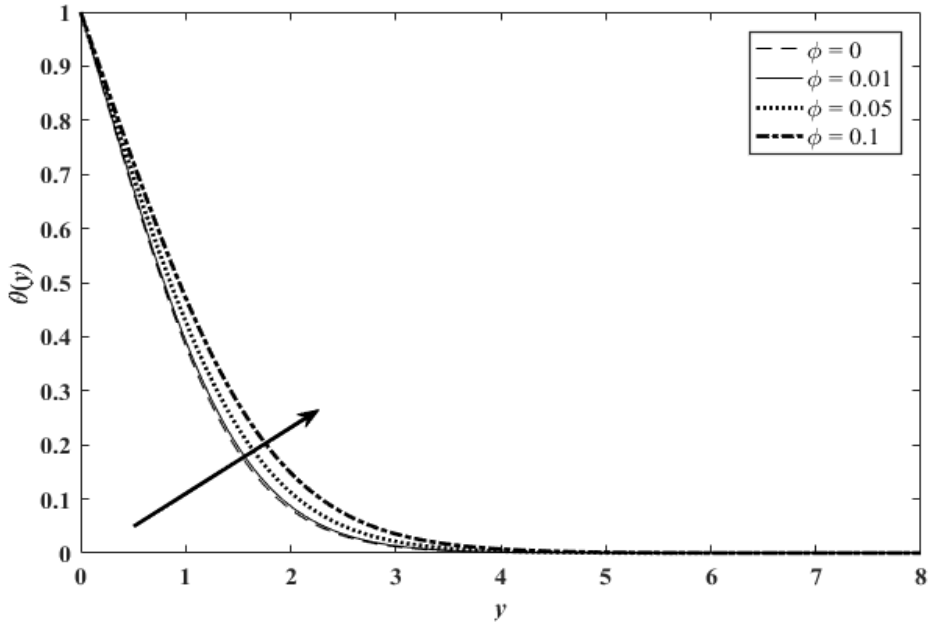

Figure 3. Temperature profile, $\theta(y)$ for increasing the ferroparticles volume fraction, ϕ when $M=1$.

The effect of magnetic parameter on velocity profile and temperature profile are shown in figure 4 and 5 respectively. It can be seen that the magnetic parameter is enlarging, where the velocity of ferrofluid and momentum boundary layer thickness has diminished as depicted in figure 4. These results were confirmed and similar as reported by Malekzadeh et al. [34] where the increase of magnetic field strength has a major impaction on the viscosity of ferrofluid. The increment of viscosity of ferrofluid causes the velocity of ferrofluid to decrease. The state of increasing the magnetic parameter is different from the situation occurs in ferroparticles volume fraction as the temperature and viscosity are dependent on each other. Conversely, increasing the magnetic parameter has an influence on the Lorentz force. The vertical y-direction of magnetic field which generated the Lorentz force in the horizontal x-direction

has the same magnetic domain [37]. The Lorentz force leads to the suppression of the fluid flow which decreases the velocity of ferrofluid and elevates the temperature of ferrofluid as shown in figure 4 and 5, respectively. Besides, the increment of magnetic parameter also elevates the thermal boundary layer and the thermal conductivity of ferrofluid as discovered by Haiza et al. [6] in their experimental study.

The magnetic strength and the ferroparticles volume fraction parameter of ferrofluid are observed further in the ratio of convective heat transfer over conduction heat transfer or called the reduced Nusselt number. The reduced Nusselt number is calculated using the equation (21) to measure the convective heat transfer at the surface as plotted in figure 6. Figure 6 shows that the reduced Nusselt number has been decreased by applying the magnetic field. From the physical view, the Lorentz force that is produced when magnetic parameter increases have a normal direction to the buoyancy force which retards the heat transfer and fluid flow [37]. These phenomena cause the suppression of the fluid movement and has tendency to control the cooling rate of the surface. On the other hand, the variation of ferroparticles volume fraction shows the reduced Nusselt number in decreasing trends along with the increase of the magnetic parameter and ferroparticles volume fraction.

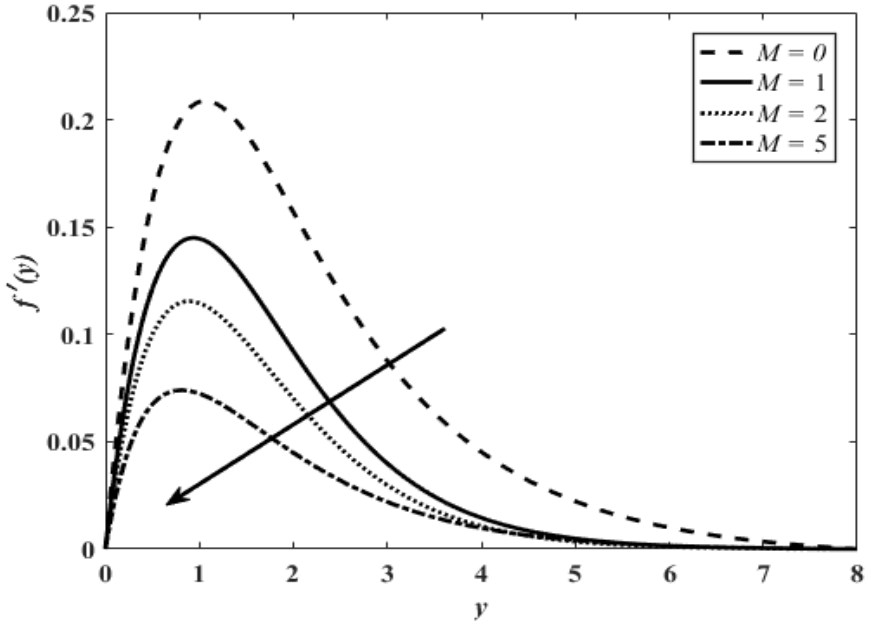

Figure 4. Velocity profile $f'(y)$, for increasing magnetic parameter, M when $\phi = 0.1$.

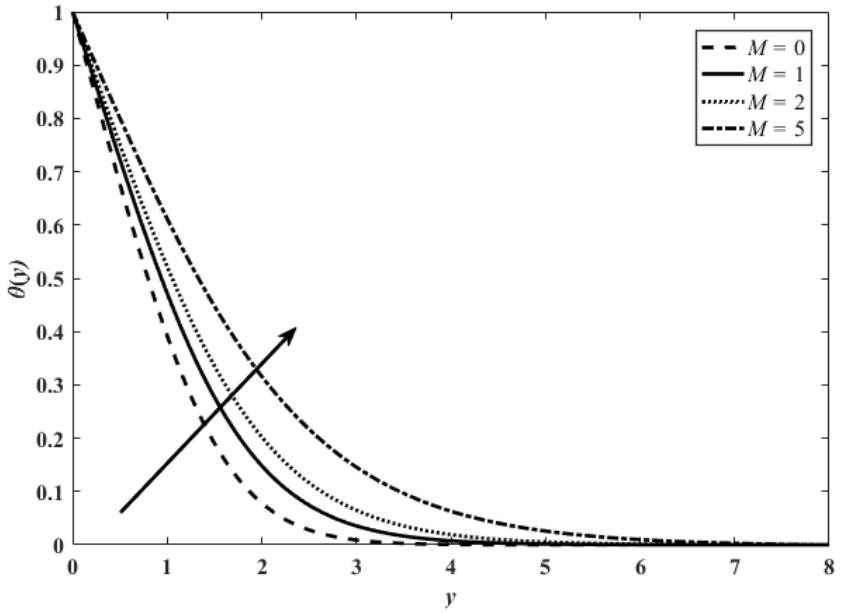

Figure 5. Temperature profile $\theta(\eta)$, for increasing magnetic parameter, M when $\phi = 0.1$.

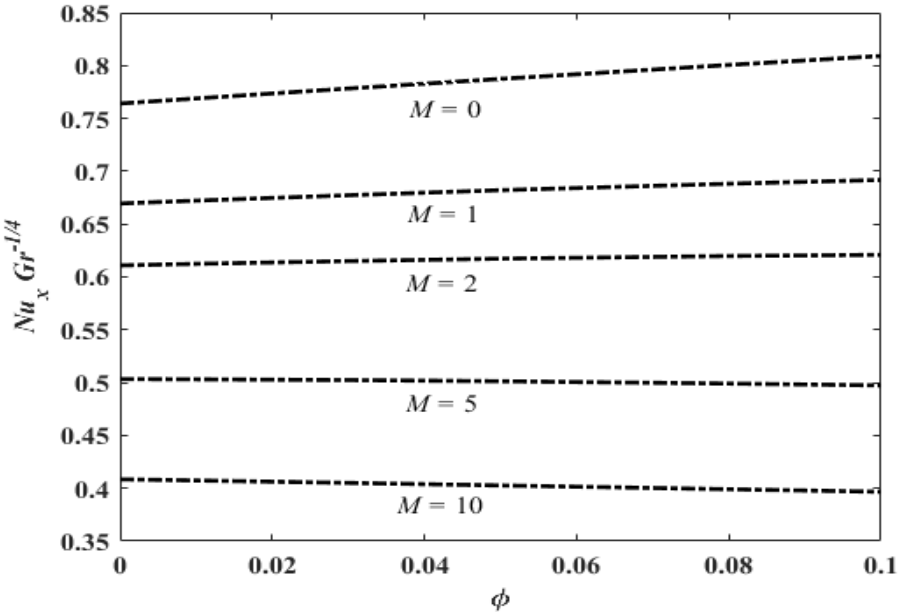

Figure 6. Variation of $Nu_x Gr^{-1/4}$ for several values of ferroparticles volume fraction, ϕ and magnetic parameter, M.

4. Conclusions

In this study, the magnetohydrodynamic (MHD) free convection flow at the lower stagnation point of a horizontal circular cylinder with the influence of an external magnetic field on ferrofluid flow and heat transfer characteristics have been investigated. The results revealed that by changing the strength of magnetic parameter and the ferroparticles volume fraction, it is not impossible to alter the thermophysical properties of ferrofluid. It is proven that the viscosity of ferrofluid changes with the

temperature when the ferroparicles volume fraction increases or decreases. The viscosity of ferrofluid increases when the ferroparticles volume fraction increases while it decreases with an increase in the temperature. Consequently, the thermal conductivity is enhanced and the velocity of ferrofluid increases. In ensuring a stable control over the fluid flow and the heat transfer, the external magnetic field needs to be applied to the lower stagnation point of horizontal circular cylinder hot surface. The magnetic field that produces the Lorentz force and the interaction with buoyancy force acts as a determiner of the trend of reduced Nusselt number, temperature and velocity of ferrofluid. With the increase of magnetic parameter, the domination of the Lorentz force starts to take place which leads to a slower flow and subsequently increases the temperature and further leads to the drop of reduced Nusselt number.

Acknowledgements
The author would like to acknowledge the Universiti Malaysia Pahang for the financial supported from the grant RDU190356 and RDU170358.

References

[1] Choi S U S and Eastman J A 1995 Enhancing thermal conductivity of fluids with nanoparticles *In Proc. Conf. on ASME International Mechanical Engineering Congress & Exposition, San Francisco, USA* 99-105.
[2] Hussain S and Ahmed S E 2019 *Journal of Magnetism and Magnetic Materials* **484** 356-366
[3] Jusoh R, Nazar R and Pop I 2018 *Journal of Magnetism and Magnetic Materials* **465** 365-374
[4] Sheikholeslami M and Ganji D D 2018 *Alexandria engineering journal* **57** 49-60
[5] Valitabar M, Rahimi M and Azimi N 2019 *Heat and Mass transfer* 1-12
[6] Haiza H, Yaacob I and Azhar A Z A 2018 *Solid State Phenomena* **280** 36-42
[7] Toghraie D, Alempour S M and Afrand M 2016 *Journal of Magnetism and Magnetic Materials* **417** 243-248
[8] Papell S S, *Low viscosity magnetic fluid obtained by the colloidal suspension of magnetic particles*, Cleveland, OH: United States. NASA Lewis Research Center, 1965.
[9] Mehta J S, Kumar R, Kumar H and Garg H 2018 *Journal of Thermal Science and Engineering Applications* **10** 020801
[10] Rosensweig R E 1985 *Ferrohydrodynamics* (New York: Cambridge University Press)
[11] Berger P, Adelman N B, Beckman K J, Campbell D J, Ellis A B and Lisensky G C 1999 *Journal of Chemical Education* **76** 943-948
[12] Darus A N 1995 *Analisis pemindahan haba: Olakan* (Kuala Lumpur: Dewan Bahasa dan Pustaka)
[13] Joshi N and Sukhatme S 1971 *Journal of Heat Transfer* **93** 441-448
[14] Merkin J 1976 Free convection boundary layer on an isothermal horizontal cylinder *In Proc. Conf. on American Society of Mechanical Engineers and American Institute of Chemical Engineers, Heat Transfer Conference, St. Louis, USA*
[15] Merkin J and Pop I 1988 *Wärme-und Stoffübertragung* **22** 79-81
[16] Aldoss T, Ali Y and Al-Nimr M 1996 *Numerical Heat Transfer, Part A: Applications* **30** 379-396
[17] Aldos T and Ali Y 1997 *International Communications in Heat and Mass Transfer* **24** 683-693
[18] Tlili I, Khan W and Ramadan K 2019 *Journal of Nanofluids* **8** 179-186
[19] Mahat R, Rawi N A, Kasim A R M and Shafie S 2018 *Sains Malaysiana* **47** 1617-1623
[20] Reddy P S and Chamkha A J 2018 *Ain Shams Engineering Journal* **9** 707-716
[21] Mohamed M K A, Noar N, Salleh M Z and Ishak A 2016 *Sains Malaysiana* **45** 289-296
[22] Mabood F, Khan W and Yovanovich M 2016 *Journal of Molecular Liquids* **222** 172-180
[23] Buongiorno J 2006 *Journal of heat transfer* **128** 240-250
[24] Tiwari R K and Das M K 2007 *International Journal of Heat and Mass Transfer* **50** 2002-2018
[25] Rashad A 2017 *Journal of the Egyptian Mathematical Society* **25** 230-237

[26] Mohamed M K A, Sarif N M, Kasim A R M, Noar N, Salleh M Z and Ishak A 2016 *ARPN Journal of Engineering and Applied Sciences* **11** 7258-7263
[27] Azim N H M A 2014 *SOP Transactions on Applied Physics* **1** 1-11
[28] Khan Z H, Khan W A, Qasim M and Shah I A 2014 *IEEE Transactions on Nanotechnology* **13** 35-40
[29] Ilias M R, Rawi N A and Shafie S 2017 *Journal of Mechanical Engineering* **14** 1-15
[30] Gibanov N S, Sheremet M A, Oztop H F and Abu-Hamdeh N 2017 *International Journal of Heat and Mass Transfer* **114** 1086-1097
[31] Sheikholeslami M and Rashidi M M 2015 *Journal of the Taiwan Institute of Chemical Engineers* **56** 6-15
[32] Tham L, Nazar R and Pop I 2012 *International Journal of Numerical Methods for Heat & Fluid Flow* **22** 576-606
[33] Zokri S M, Arifin N S, Mohamed M K A, Kasim A R M, Mohammad N F and Salleh M Z 2018 *Malaysian Journal of Fundamental and Applied Sciences* **14** 40-47
[34] Malekzadeh A, Pouranfard A, Hatami N, Banari A K and Rahimi M 2016 *Journal of Applied Fluid Mechanics* **9**
[35] Mishra P C, Mukherjee S, Nayak S K and Panda A 2014 *International nano letters* **4** 109-120
[36] Sundar L S, Singh M K and Sousa A C 2013 *International Communications in Heat and Mass Transfer* **44** 7-14
[37] Singh R J and Gohil T B 2019 *Computers & Fluids* **179** 476-489